Journal of Power Sources 189 (2009) 2–8

Contents lists available at ScienceDirect

Journal of Power Sources

journal homepage: www.elsevier.com/locate/jpowsour

Effect of Ag additive on the performance of $LiNi_{1/3}Co_{1/3}Mn_{1/3}O_2$ cathode material for lithium ion battery

Rui Guo, Pengfei Shi*, Xinqun Cheng, Yulin Ma, Zhou Tan

School of Chemical Engineering and Technology, Harbin Institute of Technology, Harbin 150001, PR China

ARTICLE INFO

Article history:
Received 23 June 2008
Received in revised form 9 January 2009
Accepted 10 January 2009
Available online 20 January 2009

Keywords:
Lithium ion battery
Cathode material
$LiNi_{1/3}Co_{1/3}Mn_{1/3}O_2$
Ag additive
Electrochemical performance

ABSTRACT

The $LiNi_{1/3}Co_{1/3}Mn_{1/3}O_2$/Ag composite used for cathode material of lithium ion battery was prepared by thermal decomposition of $AgNO_3$ added to commercial $LiNi_{1/3}Co_{1/3}Mn_{1/3}O_2$ powders to improve the electrochemical performance of $LiNi_{1/3}Mn_{1/3}Co_{1/3}O_2$. Structure and morphology analysis showed that Ag particles were dispersed on the surface of $LiNi_{1/3}Co_{1/3}Mn_{1/3}O_2$ instead of entering the crystal structure. The results of charge–discharge tests showed that Ag additive could improve the cycle performance and high-rate discharge capability of $LiNi_{1/3}Mn_{1/3}Co_{1/3}O_2$. Extended analysis indicated that Ag was unstable in the commercial electrolyte at high potential. The improved electrochemical performance caused by Ag additive was associated not only with the enhancement of electrical conductivity of the material and the lower polarization of the cell, but also with the increased "c" parameter of $LiNi_{1/3}Mn_{1/3}Co_{1/3}O_2$ after repeated charge/discharge cycles and the compact and protective SEI layer formed on the surface of $LiNi_{1/3}Mn_{1/3}Co_{1/3}O_2$.

1. Introduction

Layered transition-metal oxide $LiNi_{1/3}Co_{1/3}Mn_{1/3}O_2$, has been extensively studied as a promising cathode material for lithium ion battery, because of its higher reversible capacity, milder thermal stability, lower cost and less toxicity than commercially used $LiCoO_2$ [1,2]. Recently, with the development of high-power consuming electric devices, more efforts have been paid on the modification of $LiNi_{1/3}Co_{1/3}Mn_{1/3}O_2$ so as to further improve its electrochemical performance, especially the high-rate capability [3–6].

During the last few years, there were some researches dealing with the silver depositing (mixing) on (with) the cathode materials such as $LiFePO_4$ [7,8], $LiCoO_2$ [9] and $LiMn_2O_4$ [10–12], and improved electrochemical performance was achieved, which was mainly ascribed to fact that the Ag additives efficiently increased the electrical conductivity of the material particles. However, Huang et al. [9] reported an undesired oxidation peak about the dissolution of silver in the first cycle of cyclic voltammograms, suggesting that silver may be unstable in the nonaqueous electrolyte system under higher potential.

In this paper, a simple thermal decomposition method was used to prepare $LiNi_{1/3}Co_{1/3}Mn_{1/3}O_2$/Ag composite and the electrochemical performance was measured. The mechanism that Ag additive improved the performances of $LiNi_{1/3}Co_{1/3}Mn_{1/3}O_2$ was studied and discussed.

2. Experimental

2.1. Preparation of the $LiNi_{1/3}Co_{1/3}Mn_{1/3}O_2$/Ag composite cathode

Commercial $LiNi_{1/3}Co_{1/3}Mn_{1/3}O_2$ powder from Best Co., China, was used to prepare the $LiNi_{1/3}Co_{1/3}Mn_{1/3}O_2$/Ag composite. $AgNO_3$ (AR) was dissolved in distilled water and then the $LiNi_{1/3}Co_{1/3}Mn_{1/3}O_2$ powders were added to the $AgNO_3$ solution to obtain a suspension. The weight ratio of $AgNO_3$ to $LiNi_{1/3}Co_{1/3}Mn_{1/3}O_2$ was 1:9. The suspension was stirred vigorously to disperse the mixture homogeneously and dried at 100 °C to evaporate the water. Then the obtained precursor powders were heated in a furnace at 500 °C for 1 h in air to obtain the $LiNi_{1/3}Co_{1/3}Mn_{1/3}O_2$/Ag composite.

The electrode was prepared by mixing the cathode material (pristine $LiNi_{1/3}Co_{1/3}Mn_{1/3}O_2$ or $LiNi_{1/3}Co_{1/3}Mn_{1/3}O_2$/Ag composite, 80 wt.%), acetylene black (10 wt.%) and polyvinylidene fluoride (PVDF) binder (10 wt.%) homogeneously in *N*-methyl pyrrolidinone (NMP), and then coating uniformly on an aluminum foil. Finally, the electrode was dried under vacuum at 120 °C for10 h and punched into disks (Φ = 14 mm) for use.

2.2. Characterization and analysis

The crystal structures of the pristine $LiNi_{1/3}Co_{1/3}Mn_{1/3}O_2$ and the $LiNi_{1/3}Co_{1/3}Mn_{1/3}O_2$/Ag composite were examined on X-ray diffractometer (D/max-rB, Rigaku) with Cu Kα radiation (λ = 1.5406 Å). The morphological features were observed by scanning electron microscope (SEM, FEI QUANTA 200, Philips) and

* Corresponding author. Tel.: +86 451 86413721; fax: +86 451 86413720.
E-mail address: pfshi@hit.edu.cn (P. Shi).

0378-7753/$ – see front matter © 2009 Elsevier B.V. All rights reserved.
doi:10.1016/j.jpowsour.2009.01.016

field-emission scanning electron microscope (FESEM, S-4700, Hitachi). The existence of Ag was confirmed by energy dispersive spectrometer (EDAX). The pristine $LiNi_{1/3}Co_{1/3}Mn_{1/3}O_2$ and the $LiNi_{1/3}Co_{1/3}Mn_{1/3}O_2$/Ag composite electrodes were analyzed by X-ray photoelectron spectroscopy (XPS) using PHI5700-ESCA with focused monochromatic Al Kα radiation (1486.6 eV).

The charge and discharge behaviors of the pristine $LiNi_{1/3}Co_{1/3}Mn_{1/3}O_2$ and the $LiNi_{1/3}Co_{1/3}Mn_{1/3}O_2$/Ag composite were examined using CR2025 coin-type cells. The cell consisted of the as-prepared cathode and a lithium metal anode separated by a porous polypropylene film. The electrolyte was 1 mol L^{-1} $LiPF_6$ in a mixed solvent of ethylene carbonate (EC), diethyl carbonate (DEC) and ethyl methyl carbonate (EMC) (1:1:1 by volume). All the cells were cycled between 2.8 and 4.4 V vs. Li/Li^+ at ambient temperature (23 ± 2 °C). The constant current and constant voltage charge (CC–CV charge) was performed galvanostatically at a current density of 20 mA g^{-1} and then potentiostatically at 4.4 V until the current density dropped to less than 2 mA g^{-1}. The discharge was performed by varying the discharge current density at 20, 80, 160, 320 and 800 mA g^{-1}. Cyclic voltammetry study was carried out on CHI720B electrochemical workstation at a scan rate of 0.2 mV s^{-1} between 2.8 and 4.7 V vs. Li/Li^+.

3. Results and discussion

3.1. Characterization of the $LiNi_{1/3}Co_{1/3}Mn_{1/3}O_2$/Ag composite

When the $AgNO_3$ and $LiNi_{1/3}Co_{1/3}Mn_{1/3}O_2$ precursor powders were calcined above 440 °C, the $AgNO_3$ would decompose as follow:

$$2AgNO_3 \rightarrow 2Ag + 2NO_2 + O_2 \quad (1)$$

The weight ratio of $AgNO_3$ and $LiNi_{1/3}Co_{1/3}Mn_{1/3}O_2$ in the precursor powders was 1:9, and the Ag content in the final $LiNi_{1/3}Co_{1/3}Mn_{1/3}O_2$/Ag composite was calculated to be 6.6 wt.%.

Fig. 1 shows the X-ray diffraction (XRD) patterns of the pristine $LiNi_{1/3}Co_{1/3}Mn_{1/3}O_2$, the $LiNi_{1/3}Co_{1/3}Mn_{1/3}O_2$/Ag composite, and the Ag pattern (PDF #04-0783) as a reference. Compared with the vertical lines that stand for the typical XRD patterns of Ag metal and the pattern of $LiNi_{1/3}Co_{1/3}Mn_{1/3}O_2$/Ag composite, only the strongest characteristic Ag (1 1 1) peak can be detected between the (0 0 6) and (0 1 2) peaks of $LiNi_{1/3}Co_{1/3}Mn_{1/3}O_2$, as the amount of Ag is small and the other characteristic peaks of Ag are almost overlapped by the peaks of $LiNi_{1/3}Co_{1/3}Mn_{1/3}O_2$. Since the radius of Ag^+ (1.26 Å) is greatly bigger than that of the Co^{3+} (0.63 Å), Ni^{2+} (0.72 Å) and Mn^{4+} (0.54 Å), if Ag is doped in the lattice of $LiNi_{1/3}Co_{1/3}Mn_{1/3}O_2$, it will lead to an increase in the lattice parameters of the sample. For this reason, the lattice parameters of all the samples were calculated from the XRD results by profile fitting method. However, the "*a*" and "*c*" values of the $LiNi_{1/3}Co_{1/3}Mn_{1/3}O_2$ in the composite, 2.8628 ± 0.0006 Å and 14.240 ± 0.004 Å, are in accordance with those of the pristine $LiNi_{1/3}Co_{1/3}Mn_{1/3}O_2$, i.e., $a = 2.8640 \pm 0.0007$ Å and $c = 14.241 \pm 0.004$ Å. It is suggested that Ag does not enter the layered structure of $LiNi_{1/3}Co_{1/3}Mn_{1/3}O_2$ [9,13] and the $LiNi_{1/3}Co_{1/3}Mn_{1/3}O_2$/Ag composite is a mixture of Ag metal and $LiNi_{1/3}Co_{1/3}Mn_{1/3}O_2$.

The SEM images of the pristine $LiNi_{1/3}Co_{1/3}Mn_{1/3}O_2$ and the $LiNi_{1/3}Co_{1/3}Mn_{1/3}O_2$/Ag composite are shown in Fig. 2. Compared with the images of $LiNi_{1/3}Co_{1/3}Mn_{1/3}O_2$ and $LiNi_{1/3}Co_{1/3}Mn_{1/3}O_2$/Ag composite, it can be seen that some small irregular shaped particles with a size about several hundred nanometers exist on the surface of $LiNi_{1/3}Co_{1/3}Mn_{1/3}O_2$ particles. The energy dispersive spectroscopy (EDS) on one of the particles at the cross point (Fig. 2c) indicates that these small particles are Ag.

3.2. Electrochemical performances of $LiNi_{1/3}Co_{1/3}Mn_{1/3}O_2$/Ag composite

Fig. 3 presents the cycle performance curves of the pristine $LiNi_{1/3}Co_{1/3}Mn_{1/3}O_2$ and the $LiNi_{1/3}Co_{1/3}Mn_{1/3}O_2$/Ag composite cycled at a current density of 20 mA g^{-1} over the voltage range of 2.8–4.4 V. For the pristine $LiNi_{1/3}Co_{1/3}Mn_{1/3}O_2$, the initial discharge capacity is 165 mAh g^{-1} and the discharge capacity fades to 143 mAh g^{-1} after 50 cycles, corresponding to a capacity retention of 86.7%. For the $LiNi_{1/3}Co_{1/3}Mn_{1/3}O_2$/Ag composite, the initial discharge capacity is 169 mAh g^{-1}, which is a little higher than that of the pristine $LiNi_{1/3}Co_{1/3}Mn_{1/3}O_2$. However, the 50th discharge capacity of the $LiNi_{1/3}Co_{1/3}Mn_{1/3}O_2$/Ag composite still keeps 160 mAh g^{-1}, which corresponds to 94.7% of the initial capacity. It is evident that Ag additive can significantly improve the cycle performance of $LiNi_{1/3}Co_{1/3}Mn_{1/3}O_2$.

Fig. 4 displays the discharge capacity retention of the pristine $LiNi_{1/3}Co_{1/3}Mn_{1/3}O_2$ and the $LiNi_{1/3}Co_{1/3}Mn_{1/3}O_2$/Ag composite

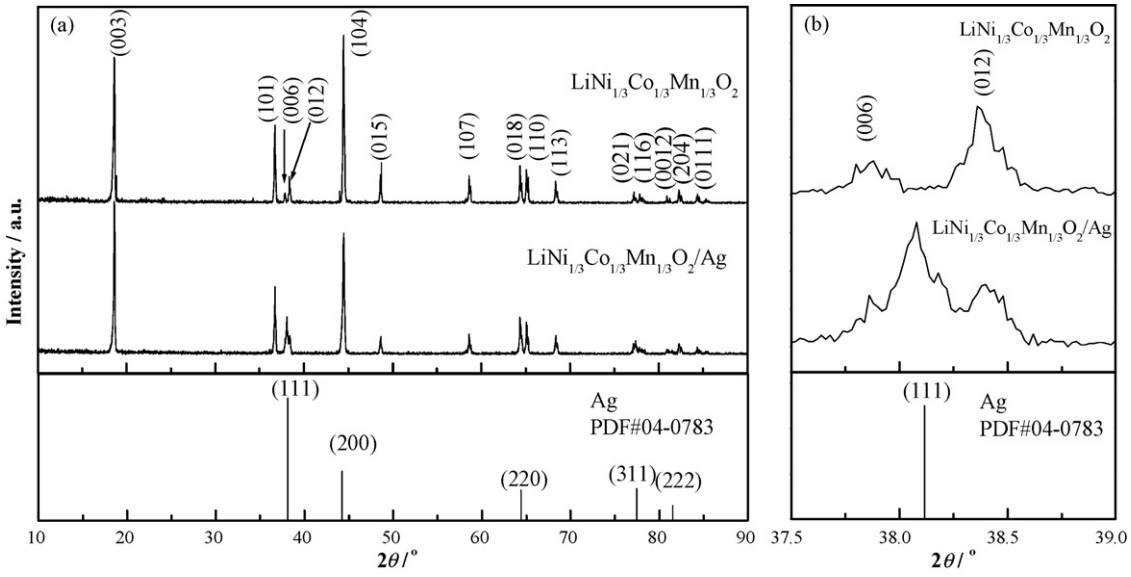

Fig. 1. (a) XRD patterns of the pristine $LiNi_{1/3}Co_{1/3}Mn_{1/3}O_2$, the $LiNi_{1/3}Co_{1/3}Mn_{1/3}O_2$/Ag composite, and the Ag pattern (PDF #04-0783) and (b) local view of (a) in the 2θ range of 37.5°–39.0°.

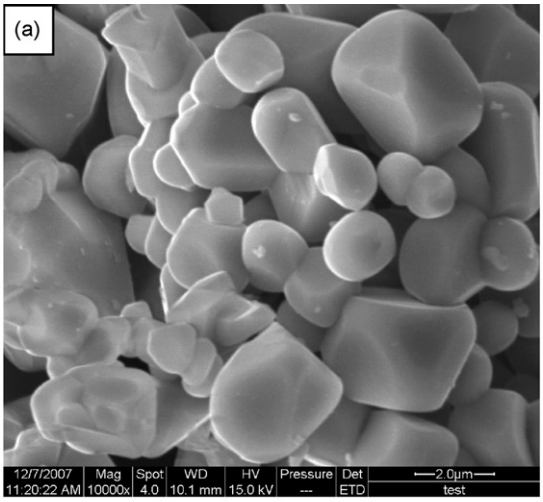

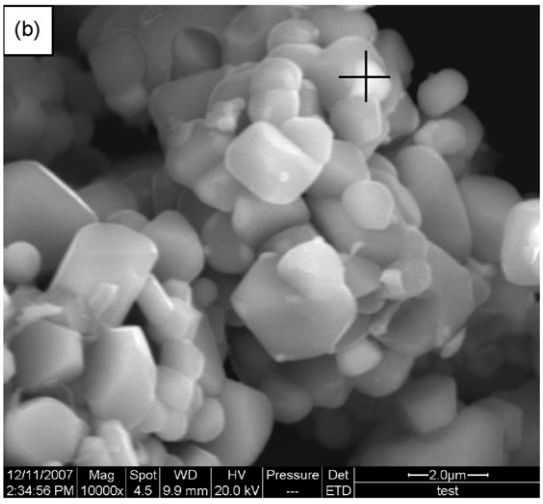

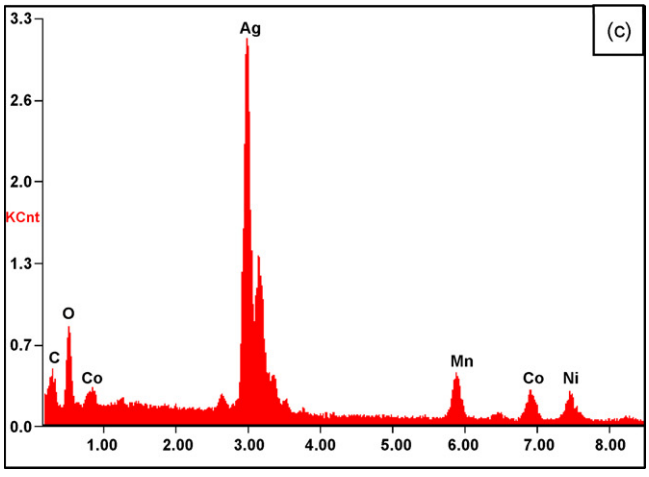

Fig. 2. SEM images of (a) the pristine $LiNi_{1/3}Co_{1/3}Mn_{1/3}O_2$, (b) the $LiNi_{1/3}Co_{1/3}Mn_{1/3}O_2$/Ag composite and (c) EDAX analysis of $LiNi_{1/3}Co_{1/3}Mn_{1/3}O_2$/Ag composite at the cross point.

cycled at various discharge current densities over the voltage range of 2.8–4.4 V. The discharge capacities gradually decrease with increasing the applied current density for both samples. However, it is clearly observed that the $LiNi_{1/3}Co_{1/3}Mn_{1/3}O_2$/Ag composite has better rate capability than the pristine one. Especially, at the current density of 800 mA g^{-1}, the initial discharge capacity of $LiNi_{1/3}Co_{1/3}Mn_{1/3}O_2$/Ag composite is 116 mAh g^{-1}, which is 69.5% of that at 20 mA g^{-1}. Meanwhile, the pristine one

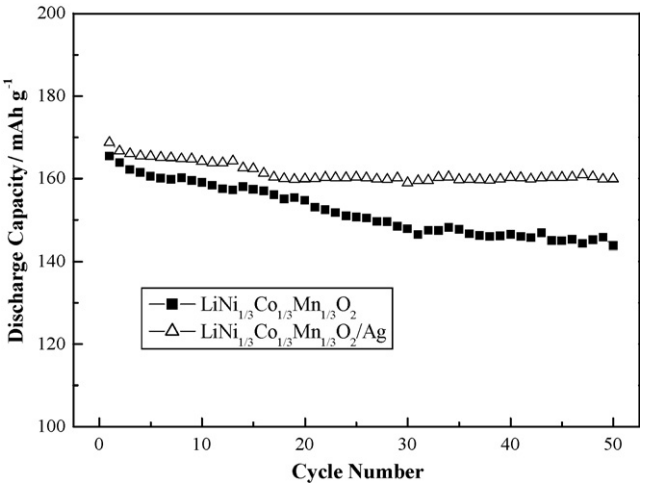

Fig. 3. Cycle performance of the pristine $LiNi_{1/3}Co_{1/3}Mn_{1/3}O_2$ and the $LiNi_{1/3}Co_{1/3}Mn_{1/3}O_2$/Ag composite at a current density of 20 mA g^{-1} over the voltage range of 2.8–4.4 V.

shows only 103 mAh g^{-1} at this current density, 62.8% of that at 20 mA g^{-1}.

3.3. Discussion on the effect of Ag additive

To further understand the mechanism of the remarkably improved electrochemical performances of the $LiNi_{1/3}Co_{1/3}Mn_{1/3}O_2$/Ag composite, the variation of Ag additive during the charge–discharge process, the structure and electrode/electrolyte interface after cycles was also studied.

The initial and cyclic voltammograms of the pristine $LiNi_{1/3}Co_{1/3}Mn_{1/3}O_2$ and the $LiNi_{1/3}Co_{1/3}Mn_{1/3}O_2$/Ag composite are displayed in Fig. 5. An additional oxidation peak at about 3.78 V was found on the initial de-intercalation curve of $LiNi_{1/3}Co_{1/3}Mn_{1/3}O_2$/Ag composite but the corresponding reduction peak was not observed. Since the potentials difference between Li^+/Li and Ag^+/Ag in the aqueous system is about 3.85 V ($Li^+ + e^- = Li$ at −3.045 V and $Ag^+ + e^- = Ag$ at 0.7991 V), this additional oxidation peak was probably attributed to the dissolution of silver [9]. Inner short circuit of the cell usually happened at the initial stage of charge while $LiNi_{1/3}Co_{1/3}Mn_{1/3}O_2$/Ag composite with higher silver content (~10 wt.%) or pure Ag powders were

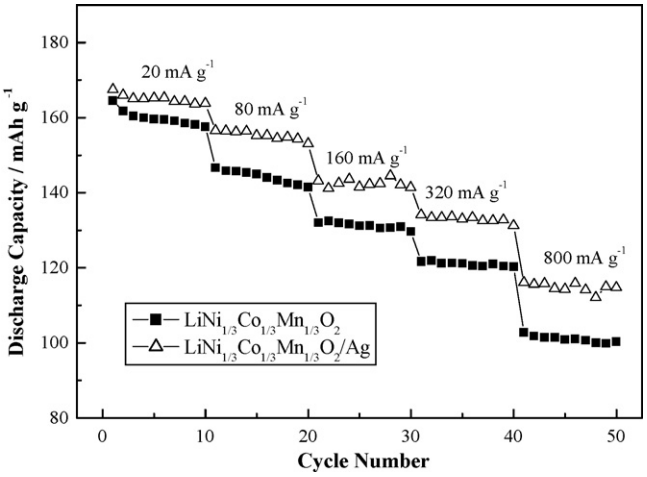

Fig. 4. The discharge capacity retention of the pristine $LiNi_{1/3}Co_{1/3}Mn_{1/3}O_2$ and the $LiNi_{1/3}Co_{1/3}Mn_{1/3}O_2$/Ag composite cycled at various discharge current densities over the voltage range of 2.8–4.4 V.

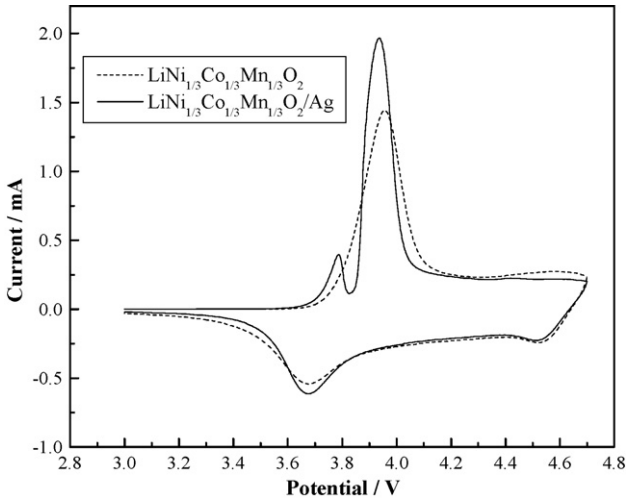

Fig. 5. Cyclic voltammograms of cells using the pristine $LiNi_{1/3}Co_{1/3}Mn_{1/3}O_2$ and the $LiNi_{1/3}Co_{1/3}Mn_{1/3}O_2$/Ag composite as the cathodes.

used as cathode. This phenomenon is due to the dissolution of silver, as the dissolved Ag deposits on the anode is the main reason caused the inner short circuit of cell. Furthermore, the dissolution of Ag happens earlier than the de-intercalation of Li^+ from the bulk of $LiNi_{1/3}Co_{1/3}Mn_{1/3}O_2$.

The initial and charge–discharge curves of the pristine $LiNi_{1/3}Co_{1/3}Mn_{1/3}O_2$ and the $LiNi_{1/3}Co_{1/3}Mn_{1/3}O_2$/Ag composite are shown in Fig. 6. It can be clearly seen that when the $LiNi_{1/3}Co_{1/3}Mn_{1/3}O_2$/Ag composite was charged to about 16 mAh g^{-1} at the beginning of the charge process, the potential of $LiNi_{1/3}Co_{1/3}Mn_{1/3}O_2$/Ag composite suddenly increases to about 3.81 V, and then falls back to normal. This phenomenon is called potential jump in following text. Comparing with the plateau of charge and discharge curves, the $LiNi_{1/3}Co_{1/3}Mn_{1/3}O_2$/Ag composite has lower polarization than the pristine $LiNi_{1/3}Co_{1/3}Mn_{1/3}O_2$. For $LiNi_{1/3}Co_{1/3}Mn_{1/3}O_2$/Ag composite, the increasing amount of the charge capacity (about 18 mAh g^{-1}) is approximately equal to the capacity before the potential jump happens. Combining with the result of cyclic voltammetry test, the dissolution of Ag happens earlier than the de-intercalation of Li^+, we presume that the increase in charge capacity is mainly due to the dissolution of silver

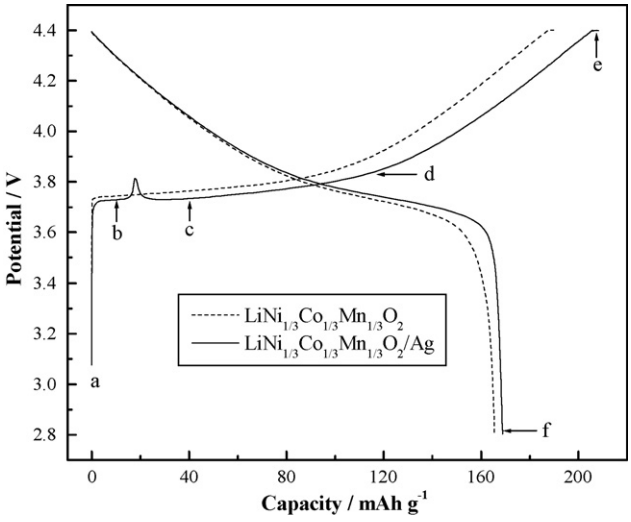

Fig. 6. The initial charge–discharge curves for the pristine $LiNi_{1/3}Co_{1/3}Mn_{1/3}O_2$ and the $LiNi_{1/3}Co_{1/3}Mn_{1/3}O_2$/Ag composite at a current density of 20 mA g^{-1} over the voltage range of 2.8–4.4 V.

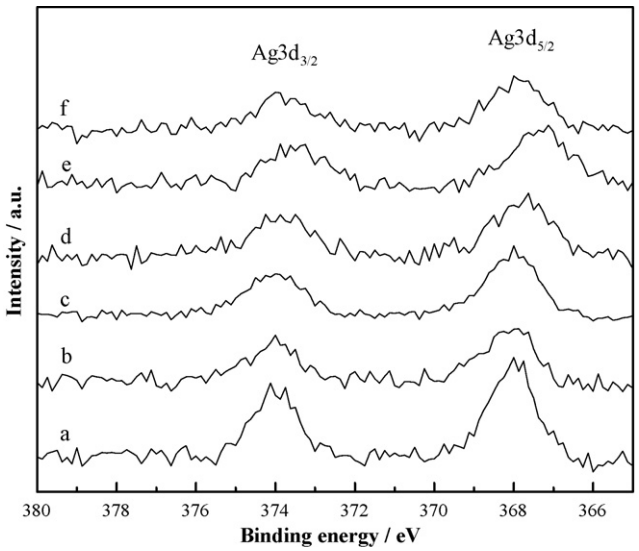

Fig. 7. Ag 3d spectra of the $LiNi_{1/3}Co_{1/3}Mn_{1/3}O_2$/Ag composite electrode at different points (a–f) on the initial charge–discharge curve: (a) before charge, (b) charged to about 3.73 V (10 mAh g^{-1}), (c) charged to about 3.73 V (40 mAh g^{-1}), (d) charged to 3.83 V, (e) charged to 4.4 V and (f) discharged to 2.8 V (after 1 cycle).

and the sudden potential jump may be associated with the end of silver dissolution.

XPS test was conducted when the $LiNi_{1/3}Co_{1/3}Mn_{1/3}O_2$/Ag composite electrode was charged and discharged to the potential at different points (from a–f) on the initial charge–discharge curve in order to investigate the valence change of Ag during the initial charge–discharge cycle, and the Ag 3d spectra were shown in Fig. 7. The binding energy of Ag $3d_{5/2}$ for the $LiNi_{1/3}Co_{1/3}Mn_{1/3}O_2$/Ag electrode before charge (a) and before the potential jump (b) is 368.0 eV, indicating that the Ag exists as elementary substance [14,15]. When the $LiNi_{1/3}Co_{1/3}Mn_{1/3}O_2$/Ag composite electrode began to charge to a lower potential after the potential jump (c), the binding energy of Ag $3d_{5/2}$ remained constant (about 368.0 eV). It indicates that some silver may still remain on the surface of the $LiNi_{1/3}Co_{1/3}Mn_{1/3}O_2$ particles after the end of silver dissolution. The reason for the appearance of sudden potential jump and the residue of silver still needs further study. When the $LiNi_{1/3}Co_{1/3}Mn_{1/3}O_2$/Ag composite electrode was at higher potential (3.83 V (d) and 4.4 V (e)), the binding energies of Ag $3d_{5/2}$ were found to be 367.6 and 367.3 eV, which are more negative than that at the beginning of charge. Since the binding energies of 367.6–367.8 and 367.2–367.4 eV were reported for Ag_2O and AgO, respectively [14–17], it is concluded that the residual Ag was further oxidized at higher potential. However, after the electrode was discharged to 2.8 V (f), the binding energy of Ag $3d_{5/2}$ increases to 368.0 eV again, this means that the oxidized Ag was reduced to Ag again or Ag was deposited back from the electrolyte. The content of Ag in the composite after one cycle must be very low, because the corresponding peak about the reduction of Ag^+ is hardly detected on the cyclic voltammogram of the $LiNi_{1/3}Co_{1/3}Mn_{1/3}O_2$/Ag composite.

Generally, the improved the electrochemical performance of the cathode with Ag mixed or coated is attribute to the enhanced surface electrical conductivity of the particles [7–10], then lower the cell polarization [10,11] and reduce the resistance [7,11,12]. Therefore, according to the results above, the existence of conductive residual Ag metal at lower potential and even AgO at higher potential on the surface of the cathode are both beneficial to reduce the resistance and polarization of the cell. However, the dissolution of Ag from the cathode and the appearance of Ag_2O on the surface of $LiNi_{1/3}Co_{1/3}Mn_{1/3}O_2$ at a certain potential range during

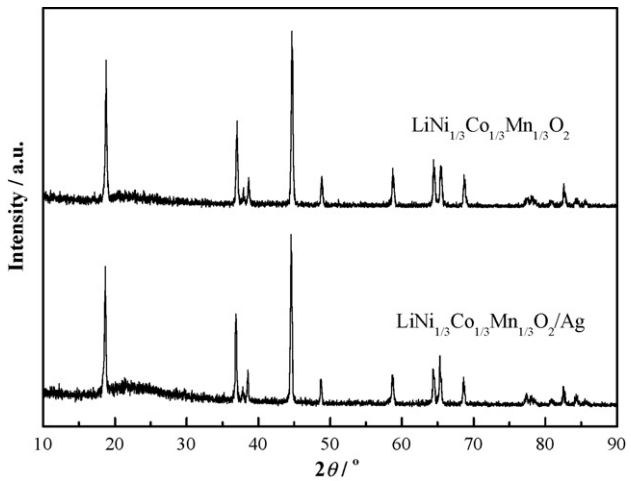

Fig. 8. XRD patterns of the pristine $LiNi_{1/3}Co_{1/3}Mn_{1/3}O_2$ and the $LiNi_{1/3}Co_{1/3}Mn_{1/3}O_2$/Ag composite at the end of discharge after 10 cycles.

the charge process will be unfavorable for increasing the electrical conductivity of the material particles. It means that the improved electrochemical performance of the $LiNi_{1/3}Co_{1/3}Mn_{1/3}O_2$/Ag composite may be not only due to the increased electrical conductivity. There may be some other reasons to improve the electrochemical performance of the $LiNi_{1/3}Co_{1/3}Mn_{1/3}O_2$/Ag composite.

XRD patterns of the pristine $LiNi_{1/3}Co_{1/3}Mn_{1/3}O_2$ and the $LiNi_{1/3}Co_{1/3}Mn_{1/3}O_2$/Ag composite at the end of discharge after 10 cycles are shown in Fig. 8. The result indicates that there is no obvious structural degradation after repeated charge/discharge cycles. The lattice parameters are: the pristine $LiNi_{1/3}Co_{1/3}Mn_{1/3}O_2$: $a = 2.851 \pm 0.001$ Å and $c = 14.252 \pm 0.005$ Å; the $LiNi_{1/3}Co_{1/3}Mn_{1/3}O_2$/Ag composite: $a = 2.8541 \pm 0.0003$ Å and $c = 14.260 \pm 0.002$ Å. It indicates that the microcosmic structure of $LiNi_{1/3}Co_{1/3}Mn_{1/3}O_2$ has changed. According to Refs. [18–20], the values of "a" and "c" have a relationship with the Li content x in delithiated $Li_xNi_{1/3}Co_{1/3}Mn_{1/3}O_2$, i.e., a-value decreases and c-value increases with the decrease of x ($x > 0.4$). The capacity consumption of the dissolution and oxidation of Ag during the initial charge process can be deducted from the initial charge (delithiation) capacity of the $LiNi_{1/3}Co_{1/3}Mn_{1/3}O_2$/Ag composite by using the Ag electrode mixed with the same amount of inert material as the $LiNi_{1/3}Co_{1/3}Mn_{1/3}O_2$ in the composite. It can be found that the initial charge (delithiation) capacity of $LiNi_{1/3}Co_{1/3}Mn_{1/3}O_2$ in the composite is similar to that of $LiNi_{1/3}Co_{1/3}Mn_{1/3}O_2$ and the 10th discharge (lithiation) capacity of $LiNi_{1/3}Co_{1/3}Mn_{1/3}O_2$/Ag is larger than $LiNi_{1/3}Co_{1/3}Mn_{1/3}O_2$, which means that the content of Li^+ in $LiNi_{1/3}Co_{1/3}Mn_{1/3}O_2$/Ag is higher than that in $LiNi_{1/3}Co_{1/3}Mn_{1/3}O_2$ after 10 cycles. Furthermore it is obvious that the contents of Li^+ are higher than 0.4 in both cycled samples. Therefore, a-value of $LiNi_{1/3}Co_{1/3}Mn_{1/3}O_2$/Ag should be larger than that of $LiNi_{1/3}Co_{1/3}Mn_{1/3}O_2$, and c-value should be lower than that of $LiNi_{1/3}Co_{1/3}Mn_{1/3}O_2$. In fact, $LiNi_{1/3}Co_{1/3}Mn_{1/3}O_2$/Ag shows a larger c-value than $LiNi_{1/3}Co_{1/3}Mn_{1/3}O_2$, which suggests a small quantity of Ag^+ might migrate into the lattice of $LiNi_{1/3}Co_{1/3}Mn_{1/3}O_2$ and expand "c" parameter of $LiNi_{1/3}Co_{1/3}Mn_{1/3}O_2$ during the repeated charge and discharge process in $LiNi_{1/3}Co_{1/3}Mn_{1/3}O_2$/Ag composite. This result indicates that Ag additive may increase the interlayer spacing of $LiNi_{1/3}Co_{1/3}Mn_{1/3}O_2$, which can facilitate the intercalation and de-intercalation of Li^+ ion [21] and be also favorable for the electrochemical performance.

Generally, the components of electrolyte can be oxidized and decomposed on the surface of the cathode materials to form solid electrolyte interface (SEI) layer, causing the change of the morphology and surface elemental components of the cycled cathode material particles [22,23]. Fig. 9 shows FESEM images of the uncycled $LiNi_{1/3}Co_{1/3}Mn_{1/3}O_2$ electrode, the pristine $LiNi_{1/3}Co_{1/3}Mn_{1/3}O_2$ and the $LiNi_{1/3}Co_{1/3}Mn_{1/3}O_2$/Ag composite electrode after 10 cycles. There are some defects on the surface of the original $LiNi_{1/3}Co_{1/3}Mn_{1/3}O_2$ particles, and the morphology of the two cycled electrodes is quite different form the uncycled one. It can be seen that the surface of all particles after 10 cycles becomes rough and may be covered by the decomposition products of the electrolyte (SEI layer). The electrolyte decomposition products on the surface of the pristine $LiNi_{1/3}Co_{1/3}Mn_{1/3}O_2$ particle are discontinuous and cannot cover the whole surface of the particles, and the surface defects are found to have an increas-

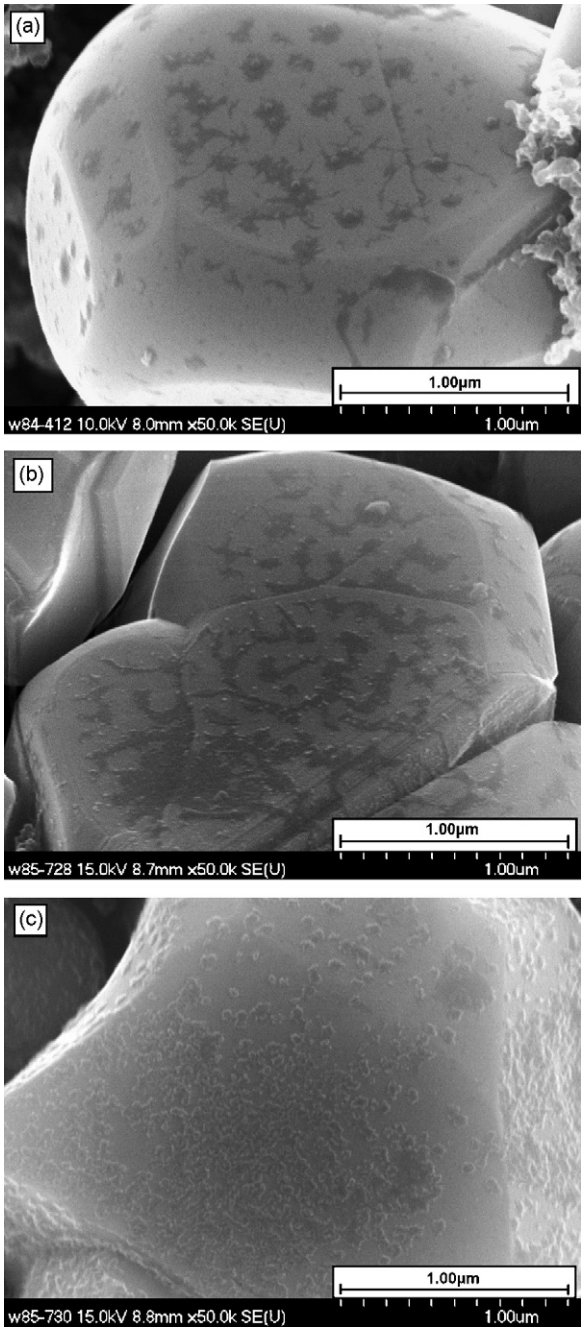

Fig. 9. FESEM images of (a) the uncycled $LiNi_{1/3}Co_{1/3}Mn_{1/3}O_2$ electrode, (b) the pristine $LiNi_{1/3}Co_{1/3}Mn_{1/3}O_2$ electrode after 10 cycles and (c) the $LiNi_{1/3}Co_{1/3}Mn_{1/3}O_2$/Ag composite electrode after 10 cycles.

ing trend compared with the original $LiNi_{1/3}Co_{1/3}Mn_{1/3}O_2$ particle before charge, which may be eroded by the electrolyte. However, the electrolyte decomposition products on the surface of the $LiNi_{1/3}Co_{1/3}Mn_{1/3}O_2$/Ag composite particle are more compact than the pristine $LiNi_{1/3}Co_{1/3}Mn_{1/3}O_2$ particle and the surface defects are hardly to be observed. It means that Ag additive can promote the decomposition of the electrolyte and the formation of more compact SEI layer.

To characterize the difference of the SEI layer formed on the surface of the pristine $LiNi_{1/3}Co_{1/3}Mn_{1/3}O_2$ and the $LiNi_{1/3}Co_{1/3}Mn_{1/3}O_2$/Ag composite electrode, XPS test was performed on these electrodes after 10 cycles and the C 1s, O 1s and F 1s spectra are shown in Fig. 10. In the C 1s spectra, the peak around 290 eV is very complicated and can be assigned to carbonate, such as Li_2CO_3 and/or RCH_2OCO_2Li [24,25], and PVDF binder $[-(CF_2CH_2)_x-]$ [22]. The broad peak around 284–288 eV is in fact a group of superimposed peaks including the graphitic carbon (contribution from acetylene black) at 284.3 eV, hydrocarbon (CH_2) peak at 285 eV, ethereal or alcoholic carbon (PEO or RCH_2OCO_2Li) around 285–287 eV [25,26] and ester carbon (RCOOR′) around 288–289 eV [26]. The O 1s spectra includes a broad peak around 531–534 eV which is attributable to carbonate (531–532 eV) and/or ethereal oxygen (533–534 eV) as the major peak [22,25], and another oxygen peak around 529–530 eV which is mainly attributable to M—O (M=Ni, Co, Mn, Li) bonds of $LiNi_{1/3}Co_{1/3}Mn_{1/3}O_2$ [27]. Because of the dissolution of Ag during repeated cycles, the increase of the decomposition products of electrolyte and the restriction of investigation depth of XPS, the signal of Ag was very weak after 10 charge–discharge cycles. It is difficult to determine the existence of Ag—O in the Ag 3d spectrum. Even though there were some Ag—O bonds in the lattice, the Ag—O component in O 1s spectrum can be ignored compared with the massive Ni—O, Co—O, Mn—O bonds in the material and decomposition products of electrolyte. In the F 1s spectra, the main peak around 688 eV is assigned to PVDF binder [22] and the shoulder peak around 685–686 eV is assigned to LiF [24,25].

The C 1s, O 1s and F 1s spectra in Fig. 10 were deconvolved by the components summarized above and the atomic percentages (%) of each component are summarized in Table 1. Comparing with the calculated results, the contents of the respective components of the $LiNi_{1/3}Co_{1/3}Mn_{1/3}O_2$/Ag composite electrode are quite different from that of the pristine $LiNi_{1/3}Co_{1/3}Mn_{1/3}O_2$ electrode. The components associated with the electrode itself (acetylene black, PVDF, and the M—O bonds) of the $LiNi_{1/3}Co_{1/3}Mn_{1/3}O_2$/Ag composite electrode are of an obviously lower content than that of the pristine $LiNi_{1/3}Co_{1/3}Mn_{1/3}O_2$ electrode. Correspondingly, the contents of the components associated with the SEI layer (RCH_2OCO_2Li, PEO, LiF, Li_2CO_3 and so on) are higher for the $LiNi_{1/3}Co_{1/3}Mn_{1/3}O_2$/Ag composite electrode. It also suggests that Ag additive can promote decomposition of the electrolyte and the formation of SEI layer, which is consistent with the SEM results. Generally, the erosion and dissolution of the cathode material caused by the electrolyte with trace HF is one of the reasons that deteriorate the electrochemical performance of the cathode materials [28]. Compact SEI layer on the $LiNi_{1/3}Co_{1/3}Mn_{1/3}O_2$ particle is beneficial to suppress the surface erosion caused by the electrolyte and improve the cyclic stability of the electrode.

Table 1
Binding energy (eV) and atomic percentage (%) of the main components of the pristine $LiNi_{1/3}Co_{1/3}Mn_{1/3}O_2$ electrode and the $LiNi_{1/3}Co_{1/3}Mn_{1/3}O_2$/Ag composite electrode after 10 cycles.

	$LiNi_{1/3}Co_{1/3}Mn_{1/3}O_2$		$LiNi_{1/3}Co_{1/3}Mn_{1/3}O_2$/Ag	
	BE/eV	%	BE/eV	%
C 1s	290.5	12.9	290.7	10.8
	288.7	5.1	288.7	7.2
	287.0	4.8	287.0	13.6
	285.9	22.4	285.9	21.5
	285.0	8.4	285.0	17.6
	284.3	46.4	284.3	29.3
O 1s	534.1	17.8	534.4	22.0
	533.0	23.6	533.0	34.0
	531.6	36.5	531.6	26.1
	529.7	22.1	529.4	17.9
F 1s	688.0	91.1	688.2	66.3
	685.5	8.9	685.5	33.7

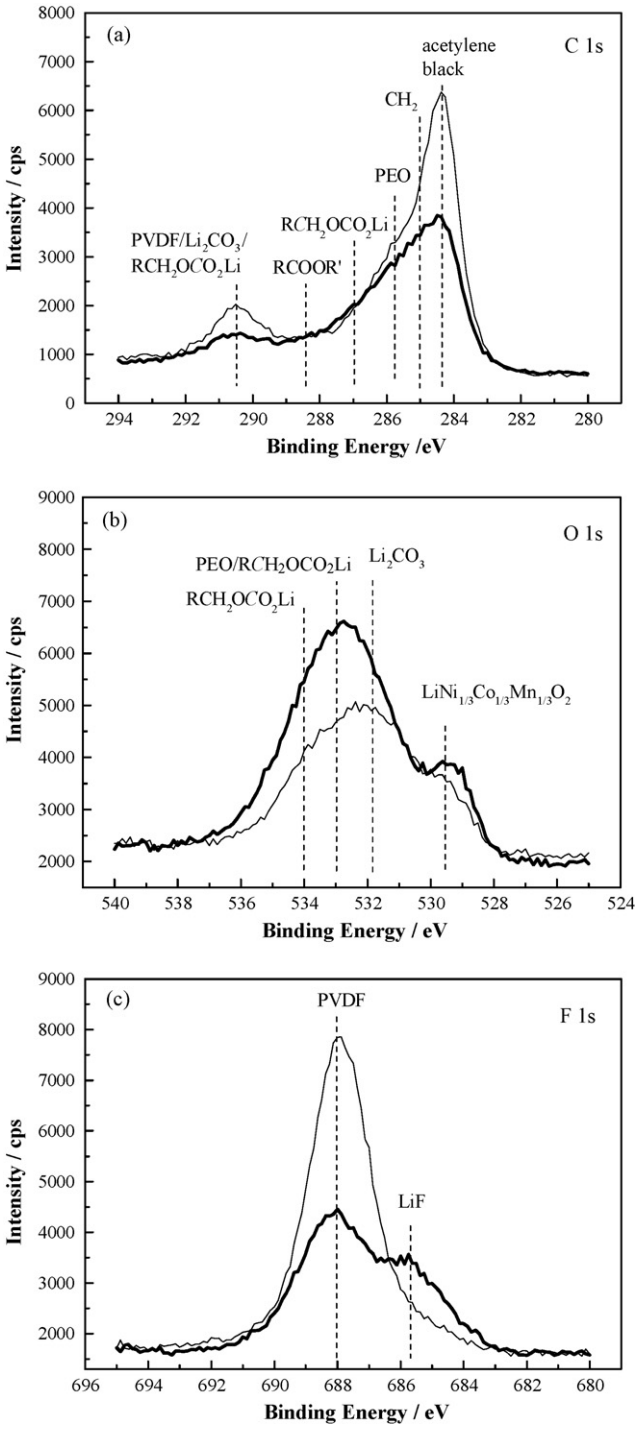

Fig. 10. C 1s, O 1s and F 1s spectra of the pristine $LiNi_{1/3}Co_{1/3}Mn_{1/3}O_2$ electrode (thin line) and the $LiNi_{1/3}Co_{1/3}Mn_{1/3}O_2$/Ag composite electrode (thick line) after 10 cycles.

4. Conclusions

The $LiNi_{1/3}Co_{1/3}Mn_{1/3}O_2$/Ag composite was successfully prepared by thermal decomposition of $AgNO_3$ added to the $LiNi_{1/3}Co_{1/3}Mn_{1/3}O_2$ powders. The Ag additive dispersed on the surface of $LiNi_{1/3}Co_{1/3}Mn_{1/3}O_2$ particles can indeed improve the cycle performance and high-rate discharge capability. Experiments confirm that Ag additive is unstable in the nonaqueous electrolyte system during the charge/discharge processes, because it can dissolve into the electrolyte or be oxidized to silver oxide. The Ag additive takes it effect in three ways: (1) reducing the conductivity and lower the polarization of the cell; (2) expanding "*c*" parameter of $LiNi_{1/3}Mn_{1/3}Co_{1/3}O_2$ after repeated charge/discharge cycles; (3) promoting the formation of compact and protective SEI layer.

Acknowledgement

Financial support by Harbin Coslight Group is greatly appreciated.

References

[1] T. Ohzuku, Y. Makimura, Chem. Lett. 7 (2001) 642.
[2] N. Yabuuchi, T. Ohzuku, J. Power Sources 119–121 (2003) 171.
[3] Y. Kima, H.S. Kim, S.W. Martin, Electrochim. Acta 56 (2006) 1316.
[4] H.S. Kim, M. Kong, K. Kim, I.J. Kim, H.B. Gu, J. Power Sources 171 (2007) 917.
[5] H.Y. Jun, G.D. Shu, L.G. Tie, L.Z. Hui, S.G. Yao, Mater. Chem. Phys. 106 (2007) 354.
[6] G.H. Kim, J.H. Kim, S.T. Myung, C.S. Yoon, Y.K. Sun, J. Electrochem. Soc. 152 (2005) A1707.
[7] C.H. Mi, Y.X. Cao, X.G. Zhang, X.B. Zhao, H.L. Li, Powder Technol. 181 (2008) 301.
[8] K.S. Park, J.T. Son, H.T. Chung, S.J. Kim, C.H. Lee, K.T. Kang, H.G. Kim, Solid State Commun. 129 (2004) 311.
[9] S.H. Huang, Z.Y. Wen, X.L. Yang, Z.H. Gu, X.H. Xu, J. Power Sources 148 (2005) 72.
[10] J.T. Son, K.S. Park, H.G. Kim, H.T. Chung, J. Power Sources 126 (2004) 182.
[11] X.M. Wu, S. Chen, Z.Q. He, M.Y. Ma, Z.B. Xiao, J.B. Liu, Mater. Chem. Phys. 101 (2007) 217.
[12] W.J. Zhou, B.L. He, H.L. Li, Mater. Res. Bull. 43 (2008) 2285.
[13] S.H. Huang, Z.Y. Wen, X.J. Zhu, Z.H. Gu, Electrochem. Commun. 6 (2004) 1093.
[14] L.H. Tjeng, M.B.J. Meinders, J.V. Elp, J. Ghijsen, G.A. Sawatzky, Phys. Rev., B 41 (1990) 3190.
[15] J.F. Weaver, G.B. Hoflund, J. Phys. Chem. 98 (1994) 8519.
[16] A.I. Boronin, S.V. Koscheev, K.T. Murzakhmetov, V.I. Avdeev, G.M. Zhidomirov, Appl. Surf. Sci. 165 (2000) 9.
[17] M. Bielmann, P. Schwaller, P. Ruffieux, O. Grönig, L. Schlapbach, P. Grönig, Phys. Rev., B 65 (2002) 235431.
[18] S.C. Yin, Y.H. Rho, I. Swainson, L.F. Nazar, Chem. Mater. 18 (2006) 1901.
[19] D.C. Li, T. Muta, L.Q. Zhang, M. Yoshio, H. Noguchi, J. Power Sources 132 (2004) 150.
[20] S. Miao, M. Kocher, P. Rez, B. Fultz, Y. Ozawa, R. Yazami, C.C. Ahn, J. Phys. Chem. B 109 (2005) 23473.
[21] P. Ghosh, S. Mahanty, R.N. Basu, Mater. Chem. Phys. 110 (2008) 406.
[22] A.M. Andersson, D.P. Abraham, R. Haasch, S. MacLaren, J. Liu, K. Aminea, J. Electrochem. Soc. 149 (2002) A1358.
[23] D. Aurbach, K. Gamolsky, B. Markovsky, G. Salitra, Y. Gofer, U. Heider, R. Oesten, M. Schmidt, J. Electrochem. Soc. 147 (2000) A1322.
[24] S. Naille, R. Dedryvère, H. Martinez, S. Leroy, P.E. Lippens, J.C. Jumas, D. Gonbeau, J. Power Sources 174 (2007) 1086.
[25] T. Eriksson, A.M. Andersson, A.G. Bishop, C. Gejke, T. Gustafsson, J.O. Thomas, J. Electrochem. Soc. 149 (2002) A69.
[26] R.I.R. Blyth, H. Buqa, F.P. Netzer, M.G. Ramsey, J.O. Besenhard, P. Golob, M. Winter, Appl. Surf. Sci. 167 (2000) 99.
[27] K.M. Shaju, G.V. Subba Rao, B.V.R. Chowdari, Electrochim. Acta 48 (2002) 145.
[28] M. Wohlfahrt-Mehrens, C. Vogler, J. Garche, J. Power Sources 127 (2004) 58.